Structural Analysis of Potential Dual Quasar Pairs Using Galactic Modeling Software

Daniel P. Gause

Department of Physics, Middlebury College, Middlebury, VT, 05753

(Dated: November 20, 2019)

Abstract

The study of dual quasar systems has recently been of heightened interest. Quasars are actively accreting supermassive black holes residing in the center of massive galaxies, and are one of the most luminous objects in the universe. Quasars play an important role in galactic evolution theory, and dual quasar systems have implications of altering their host galaxy properties. In this project, Hubble Space Telescope images of several selected candidate dual quasar systems will be thoroughly analyzed using GALFIT, a morphological modeling program. Point Spread Functions will be built for each source to account for optical aberrations in the various cameras aboard the Hubble Space Telescopes. Through GALFIT analysis, candidates will either be accepted as true dual quasars, or rejected as gravitational lenses, minor galaxy mergers, or other systems falsely resembling dual quasars. In addition, I will explore whether these dual quasars candidates appear to reside in a single shared host galaxy, or whether each source still retains its own host. Wither finding will set constraints on models of galaxy mergers that trigger quasar activity.

I. INTRODUCTION

Interest in the study of quasars has been consistently growing for decades. Since their discovery in the 1950s through radio astronomy, they have quickly become some of the most studied astronomical objects. These physical characteristics give them unique properties that allow us to peer deeper into space. They are some of the most luminous and oldest known interstellar objects. Through quasars, we can learn about about the large scale structure of the universe, the nature of dark matter, and the morphological evolution of galaxies. The wealth of knowledge that quasars hold is vast, and we have only begun to skim its surface.

Quasars are comprised of an accretion disk surrounding a supermassive black hole at the center of a galaxy. The mass of these black holes can range from millions to billions of times the mass of the sun. Gas, dust, and other local matter accrete around the black hole, bound by the black hole's immense gravitational force. While only a fraction of the accreted matter falls directly into the black hole, the matter has an induced angular momentum, causing it to form a rotating disk. These accretion disks are generally — to — parsecs across. The gravitational force from the black hole accelerates the accreting matter to relativistic speeds. The friction between the accelerated matter produces huge amounts of energy, leading to extreme luminosities, ranging from 10^{45} – 10^{47} ergs s^{-1}. Quasars are excellent at converting matter into energy as the process of accretion of matter onto the black hole is energy efficient – the gravitational energy release by accretion has an efficiency of 32%.[6] For reference, the nuclear fusion of hydrogen in stars has an energy release efficiency of only 0.7%. The immense luminosities from the high energy release efficiency of accreting matter is one of the unique characteristics of quasars that make their study so worthwhile. Extremely distant sources are detectable due to their high absolute magnitudes.

While all quasars have accretion disks, there are a number of morphological factors that vary between individual quasars. Some quasars have a dust torus radially beyond the accretion disk. These tori can significantly obscure the light emitted from accretion disks – especially when the quasar has an inclination angle so that the plane of the disk and torus is parallel to our line-of-sight from Earth. Some quasars also have radio synchrotron radiation jets and optical jets – narrow beams of particles travelling away from the central black hole at relativistic speeds. The matter accelerated through these jets can travel up

to a megaparsec, or roughly 3×10^{20} km. While the precise cause of jets is disputed, it is generally agreed that these jets provide a feedback mechanism for quasars. Also present in some quasar systems are large radio lobes ballooning out from the central black hole.

While certain components of quasars vary, their spectra are generally consistent and distinct. Inherent in quasar spectra are a number of characteristic absorption and emission lines corresponding to different regions of the quasar. There are recognizably broadened spectral lines and sharp, resolved spectral lines produced by broad line and narrow line regions respectively. Additionally, some quasars, known as radio loud quasars, have strong radio emission, sourcing from radio jets and lobes. There is also significant x-ray emission from the accretion disk. Quasars are tend to be old and distant objects, resulting in large redshifts of spectral lines. As quasars are old, luminous, spectrally recognizable, and regularly distributed throughout the universe, they are ideal objects for determining distance and redshifts of regions of space. Like lighthouses scattered all around us, they provide a standard of measure and scale of the biggest dimensions. Where the light from most objects of the early universe would be too dim to detect, the extreme luminosity of quasars enables us to see traces of the distant past.

The facet of interest in quasars for this study is the morphological evolution of galaxies. Every quasar is hosted by a galaxy. These galaxies are usually giant ellipticals, but there have been examples of other morphological types.[2] These galaxies tend to be large so that they can continually feed the accretion disk of the quasar. A small galaxy would not have enough disposable matter to fuel a live quasar. Additionally, as quasars tend to be at high redshifts, their host galaxies are generally older, and elliptical galaxies are thought to be one of the last stages of galactic development. There is also speculation into the role of early-stage galactic mergers in the origin of massive elliptical galaxies.[7]. The confirmation of this theory would fill an important gap in our understanding of galaxy evolution. A tangential theory draws connections between Active Galactic Nuclei (AGN) and galaxy mergers. AGN are a class of galaxies that have an ultra-luminous nucleus due to matter accreting onto a supermassive black hole. Quasars are the most luminous subcategory of AGNs. It has been shown that AGN can turn "on" or "off" much like a flashlight, transitioning between a dormant state and an actively accreting state.[1] While it is not fully understood what causes these changes, theories suggest that galaxy mergers can introduce new matter and trigger star formation that reignite dormant AGN.[3]

Dual quasar systems are an excellent tool in uncovering the mechanisms behind these theories. Dual quasars (DQSOs) are two gravitationally bound quasars in close proximity. In order to be deemed a DQSO, the two quasars must have a separation of 10 pc to 10 kpc – systems with a separation of < 10 pc are considered binary quasars.[5] These two quasars orbit around each other, and depending on their separation and host galaxy diameters, will share accreting matter. While research on DQSOs is limited, it is speculated that they form with the merger of two quasar housing host galaxies. If this theory were to be true, DQSO systems would be an important stage in galactic development, and would give critical insight into the effect of galaxy mergers on AGN activity. Observing galaxy mergers between non active galactic nuclei can be difficult, but with the increased luminosity of quasars we can pinpoint galaxy mergers at much higher redshifts. This effectively deepens our view, increasing the number of visible subjects. Additionally, with the wealth of knowledge that exists within quasar spectra, we can make more detailed speculations based on emission and absorption lines into the timelines and physical conditions of specific mergers. This information would be invaluable in clarifying galactic merger and AGN activation theories.

This past summer I worked on a research project with Glikman, Ph.D. of Middlebury College and Lindsay Graham of Wellesley College searching for DQSO systems at high redshifts. There have been relatively few confirmed DQSO systems detected to date, and the theorized density of dual quasars in space suggested the existence of many undiscovered DQSO systems. We suspected that many DQSO systems had been overlooked, and had been incorrectly labeled as single quasars. We built an algorithm that analyzed archival Hubble Space Telescope data containing the coordinates of known quasars. This image data was inspected and we ultimately found 21 strong candidate dual quasar systems. Using available volume calculations we determined that approximately 1% of the space analyzed contained a DQSO system.[10] If these candidates were to be confirmed as DQSO systems, our theory would be supported, proving that many DQSO systems have simply been overlooked. Increasing the number of known DQSOs enhances our ability to conduct research into the mechanisms behind AGN activity and long-term galaxy evolution.

In this project, four (?) DQSO candidates were selected from the 21 candidates proposed in this summer's research. In order to accept or deny the DQSO nature of these candidates, point spread functions were generated for each system, and used for mathematical luminosity modelling through GALFIT.

II. METHODS

Candidate Selection and PSF Generation

From our list of 21 candidate dual quasar systems, we had to select a subset based on common parameters. Factors considered included the specific Hubble Space Telescope camera used for each image capture, the resolution quality of each image, and the overall DQSO likelihood of each candidate. We first pared down the list by estimating the point source separation of each system. This was done using the redshift of each source, as the angular size is related to redshift by,

EQUATION (check with Glikman)

$$\Delta\theta = \tag{1}$$

To simplify the computing process, we used Ned Wright's Cosmological Calculator, a public algorithm devoted to computing times and distances as a function of redshift for user-defined cosmological parameters.[8] In the computation, we assumed a Hubble Constant of 69.6 $\frac{\text{km}}{\text{s Mpc}}$, an Omega$_M$ value of 0.286, and an Omega$_{vac}$ value of 0.714. These parameters estimate a flat, expanding universe dominated by dark matter – the most accepted current model of the universe. We extracted the redshift of each candidate system from our compiled list of quasars, and used Ned's Cosmological Calculator to compute the angular size, which was then converted to kpc per arcsecond. We then estimated the point source separation of each system in arcseconds using DS9 software, and compared this to the corresponding kpc per arcsecond scale to determine the separation in kpc.[4] We classified a candidate as promising if the separation was under 10 kpc, and unlikely if the separation was greater than 10 kpc, as per our earlier stated definition of dual quasar systems. From this subset, we selected 11 candidates that exhibited the most convincing DQSO characteristics.

We then determined the HST camera used for each candidate image capture. This information was available through the MAST HST Data Search database. The total number of sources from each HST camera can be found in Table I.

TABLE I. HST Camera Sources

HST Camera	WFC3	ACS	WFCP2	NICMOS
Counts	3	5	2	1

With this information, we then had to consider the varying techniques for generating point spread functions for each HST camera. Point spread functions are critical in observing and comparing astronomical image data. Light incident on a camera will naturally spread due to optical lens aberrations and finite pixel size. A point spread function describes the two-dimensional distribution of a point source of light across an astronomical cameras focal plane. PSFs vary widely between cameras, as each camera has a different lens and pixel data processing method. Additionally, the PSF of a single camera can vary depending on the position of the target source on the lens itself. As quasars and stars are point sources of light, generating accurate PSFs was crucial to this project. Thus, in choosing which candidate systems we would focus on, we considered the PSF generating techniques for each HST camera.

In general, PSFs are generated by sampling a subset of stars surrounding the target position in an image. By averaging the spread of light from each of these point sources, one can build a function that adequately describes the point spread of a position on a specific camera lens. While this method is reliable, it can be both tedious and time intensive. Thus, it is preferable to use existing algorithms for generating PSFs. One such algorithm is TinyTim, a software package developed by the Space Telescope Science Institute (STScI) for generating HST PSFs. TinyTim is written and distributed in C, and runs on UNIX systems. It requires the input of a FITS astronomical image file, the HST camera and detector number, the position on the focal plane of the detector, the filters used in image capture, the form of the target object's spectra, and the required PSF size. TinyTim then uses these parameters along with the specific diffraction patterns of the chosen camera to estimate a PSF through a sum of Zernike polynomials – a set of polynomials orthogonal on the unit disk.[12] Zernike polynomials are much like spherical harmonics, but are applied to two-dimensional systems.

TinyTim has PSF generating capabilities for all of the HST cameras, but with varying effectiveness. It is generally accepted that PSFs generated for the ACS and WFCP2 cameras by TinyTim are the most accurate, while the PSFs generated for the WFC3 and NICMOS cameras are of lower quality. For this reason, along with the high number of DQSO candidates with ACS image data, we decided to focus our modeling efforts on the ACS candidates. To customize the generated ACS PSFs for our analysis, we inputted a custom quasar spectrum, sourced from E. Glikman. (how to cite?) A visualization of the low end of the quasar

spectrum used can be found in Fig 1.

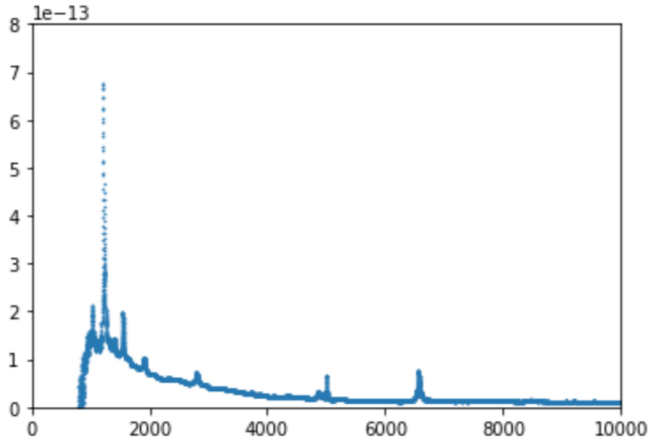

FIG. 1. Quasar spectrum used for TinyTim PSF generation. (wavelength (Å) vs flux (erg/s/cm2/A))

Multicomponent Fitting with GALFIT

After generating the PSFs for our ACS imaged DQSO candidates, we began the process of modeling. Our modeling method used the morphological modeling program, GALFIT. GALFIT is a widely used open source software package used to extract information about interstellar objects by using parametric functions to model objects as they appear in two-dimensional digital images. GALFIT takes an image file of an object, a corresponding PSF, and a set of image and function component parameters and generates a luminosity model. See Figures 2 and 3 for examples of GALFIT input files. The luminosity profiles of various astrophysical objects can be simulated through a set of analytic functions available in GALFIT. Objects such as stars and quasars have point source luminosity profiles, whereas elliptical and spiral galaxies follow Sérsic, Nuker, and other more complex profiles.

Upon the input of an image file, a PSF, and various parameters, GALFIT uses a Levenberg-Marquardt algorithm to minimize the residual between the original image and the mathematical model. The Levenberg-Marquardt algorithim, also known as the damped-least squares method (DLS), is a solution to the nonlinear least squares problem.[9] This statistical method is an iterative procedure that aims at minimizing the reduced χ^2, χ^2_ν. χ^2_ν

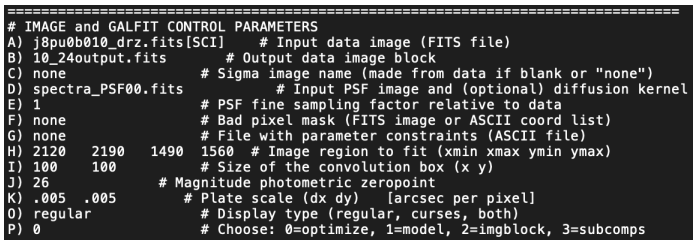

FIG. 2. An example of GALFIT image input parameters in UNIX.

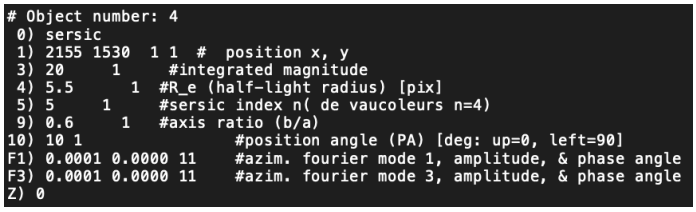

FIG. 3. An example of a GALFIT function component input in UNIX.

is defined in the standard way as

$$\chi^2_\nu = \frac{1}{N_{\rm dof}} \sum_{x=1}^{nx} \sum_{y=1}^{ny} \frac{({\rm flux}_{x,y} - {\rm model}_{x,y})^2}{\sigma^2_{x,y}} \tag{2}$$

where

$$model_{x,y} = \sum_{\nu=1}^{nf} f_{\nu,x,y}(\alpha_1 ... \alpha_n) \ . \tag{3}$$

$N_{\rm dof}$ is the number of degrees of freedom in the fit; nx and ny are the x and y image dimensions; and ${\rm flux}_{x,y}$ is the sum of the nf functions $f_{\nu,x,y}(\alpha_1 ... \alpha_n)$ employed, where $\alpha_1, ..., \alpha_n$ are the two-dimensional model parameters. GALFIT adjusts the function component parameters in small increments, iterating through models to find the model that minimizes χ^2 of the pixel intensity. The collection of components and parameters that minimizes χ^2 in GALFIT most accurately models the luminosity profile of the input image.

For each candidate DQSO source, we initially downloaded the image data from the STScI MAST Portal. This was retrieved based on each candidate's World Coordinate System (WCS) Fifth Fundamental Catalog (FK5) coordinates. We then batch downloaded all available astrodrizzed files containing that coordinate position, filtering out any uncalibrated data files. We then piped the relevant *fits* data image files into a python script that cropped the image to a 100 $\times$ 100 pixel cutout of our candidate DQSO system. This cutout was the image file we used to create our PSFs and for GALFIT fitting.

TABLE II. Candidate DQSO Systems imaged with *HST* ACS

Source Name	RA.	Dec.	Redshift	Filters	Exposure Time (s)	Zero Point Mag	Separation (kpc)
COSMJ09583+0146	149.58667	1.76917	0.785	FR716N	400	-21.1	?
				FR647N	60	-21.1	
				FR551N	500	-21.1	
4C24.10	79.01333	24.97361	0.063	FR716N	400	-21.1	0.611
				FR647N	60	-21.1	
				FR551N	500	-21.1	
COSMJ10020+0201	150.5156	2.02917	0.898	F814W	2028	-21.1	2.09
PSS J2322+1994	350.52972	19.73972	4.17	F814W	2028	-21.5	10.461

We then tested a variety of component combinations on each candidate DQSO source to determine which model best fit the system, and recorded the component parameters and χ^2 statistical values. Every candidate featured two distinct luminosity sources of varying apparent magnitudes and separations. General astrophysical information on each source can be found in Table II. A DQSO system would most likely exhibit two quasar components with PSF luminosity profiles each embedded in a host galaxy component. It is possible for two quasars to be embedded in a single host galaxy, but the resolution necessary to observe these small scale separations can be hard to attain through HST ACS images. For our sources, we used solely Sérsic functions to model host galaxy radial luminosity profiles. These profiles are given by the equation

$$\Sigma(r) = \Sigma_e \exp[-\kappa((\frac{r}{r_e})^{1/n} - 1)] \tag{4}$$

where r_e is the effective radius within which half the total flux is contained, the surface brightness at the effective radius is Σ_e, and n is the Sérsic index.[11] The value of the Sérsic index changes the modeled galaxy morphology; $n = 4$ generally represents elliptical galaxies, $n = 1$ represents spiral galaxies, and $n = 0.5$ is a two-dimensional Gaussian distribution.

We initially fitted a single PSF to each luminosity peak, representing two point sources without host galaxies. We used this model as an initial benchmark to compare more complex models to. We then layered one Sérsic component behind one of the PSFs, leaving one PSF

standing alone. This model resembles a system with a single quasar embedded in a host galaxy and a less distant line-of-sight star. We then switched the Sérsic component to the other PSF. We then replaced the stand alone PSF with a Sérsic component, modeling a system with an active AGN and a nearby galaxy with an inactive galactic nucleus. We then switched the PSF to the other Sérsic component. We then added back the second PSF, embedding each PSF in a host galaxy Sérsic radial profile. This model represented the dual quasar system we were testing for. If the source exhibited additional features, such as tidal arms or nearby extraneous luminosity sources, we adjusted our model components as we saw fit. Finally, to check for overfitting, we added an additional host galaxy Sérsic component to our model, and observed how it affected the χ^2 value. This process is visualized in a schematic in Fig 4.

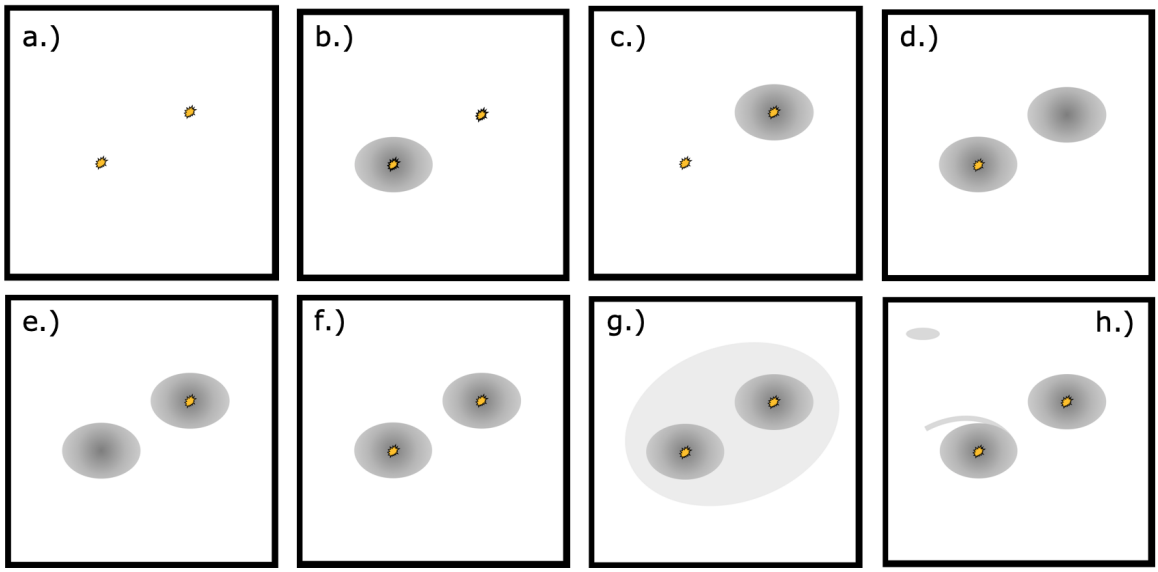

FIG. 4. Our GALFIT component modeling method. Each consecutive frame represents an additional modeling stage. The points represent PSF components, while the larger ellipses represent Sérsic components. The large ellipse in *g.*) represents an additional Sérsic component to test for overfitting. The smaller ellipse and non-symmetric arm in *h.*) represent any additional features we attempted to fit.

We compared the χ^2 values for each consecutive fit, and used an F-test to determine the improvement between modeling stages. We also used the DS9 *projection* region type to capture luminosity intensity cross-sections of each source.

III. RESULTS

We preformed the multiple stages of GALFIT analysis on three different candidates – 4C24.10, COSM J10020, and PSS J2322. We decided to focus on different modeling stages for each candidate based on the general nature of each source. The results of these fits can be found in Table III.

4C24.10

COSM J10020

For COSM J10020, we decided to complete stages (a) through (g) given in Fig 4. This source had few background artifacts in the 100 × 100 pixel cutout, allowing us to skip stage (h). Our PSF only fit produced a χ^2_ν value of 0.721. This was significantly larger than any of our following fits, but gave us a sense of appropriate magnitudes to assign each peak. The two magnitudes were 22.43 and 22.77 respectively, meaning that the two sources contributed similar luminosities to the overall luminosity profile. In the following 5 modeling stages, we saw gradual improvement in χ^2_ν values – by layering a single Sérsic component behind one of the PSFs, we reduced the χ^2_ν to 0.608. The model and residual images for fit (b) can be found in Fig. 5. Every time we added a Sérsic component, we held its position parameters constant – otherwise the Sérsic component tended to drift towards the center of the system and spread to account for more luminosity. By holding the position parameters constant, we retained the effect of modeling two individual galaxies. Our final fit, (f), had the significantly lowest χ^2_ν value of 0.521. This fit included two PSFs, each embedded in a host galaxy. The model and residual images for fit (f) can be found in Fig. 6.

Fit (f) having the lowest χ^2_ν value is good evidence for the confirmation of dual quasar characteristics.

f-test

TABLE I. Candidate DQSO Systems imaged with *HST* ACS

Source Name	Model Type	Y_{PSF1} (mag)	Y_{PSF2} (mag)	Y_1 (mag)	Y_2 (mag)	R_{e1} (pixels)	R_{e2} (pixels)	n_1	n_2	χ^2	ν ($N_{\rm DOF}$)	χ^2_ν
4C24.10 (FR716N)	a.)	18.16	18.09	...	...	...	...	...	...	7447.22	10194	0.731
comp	b.)	18.29	18.28	14.61	...	83.66	...	2.04	...	6432.29	10185	0.632
comp	h.)	18.16 (20.04)	18.10 (20.50)	...	...	...	...	...	...	7365.356	10188	0.723
comp	h.)	19.86 (20.03)	20.37 (20.56)	17.04	16.90	3.70	3.70	5.05	4.45	6689.47	10172	0.658
COSM J10020	a.)	22.43	22.77	...	...	...	...	...	...	3882.99	5034	0.721
comp	b.)	22.99	23.382	21.31	...	5.64	...	0.974	...			
comp	c.)	22.98	23.30	...	24.31	...	5.22	...	0.95	2702.28	5025	0.538
comp	d.)	28.83	...	21.0	22.01	2.99	2.46	3.19	2.78	2679.13	5019	0.534
comp	e.)	...	22.96	21.88	21.83	4.75	2.74	1.11	3.25	2623.08	5019	0.523
comp	f.)	23.00	23.84	21.78	22.15	4.71	3.30	1.14	2.57	2612.77	5016	0.521
PSS J2322	a.)	20.73	18.66	...	...	...	...	...	...	7532.8	10914	0.739
comp	b.)	18.89	20.73	20.04	...	0.17	...	10.81	...	7011.58	10185	0.688
comp	c.)	18.65	21.42	...	20.50	...	0.155	...	19.99*	9040.19	10185	0.888
comp	d.)	18.66	...	21.18	21.29	1.29	0.18	4.2	0.58	7302.13	10179	0.717
comp	e.)	...	21.42	18.57	21.32	0.01	0.70	4.54	0.04	26830.12	6179	2.636
comp	f.)	18.66	21.22	19.67	21.24	0.01	1.01	15.69	10.09	7161.34	10176	0.704
comp	h.) 18.66	20.75 (25.44)**		22.07		16.02		2.76		6865.20	10182	0.674

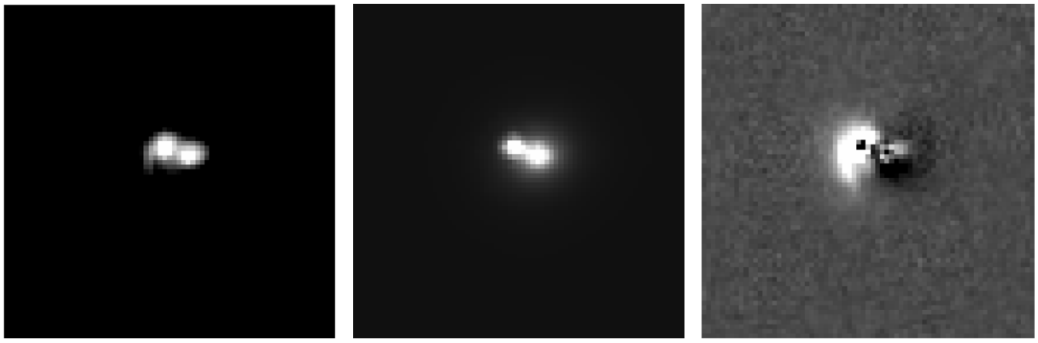

FIG. 5. The COSM J10020 source, the GALFIT produced model using fit stage (b), and the corresponding residual.

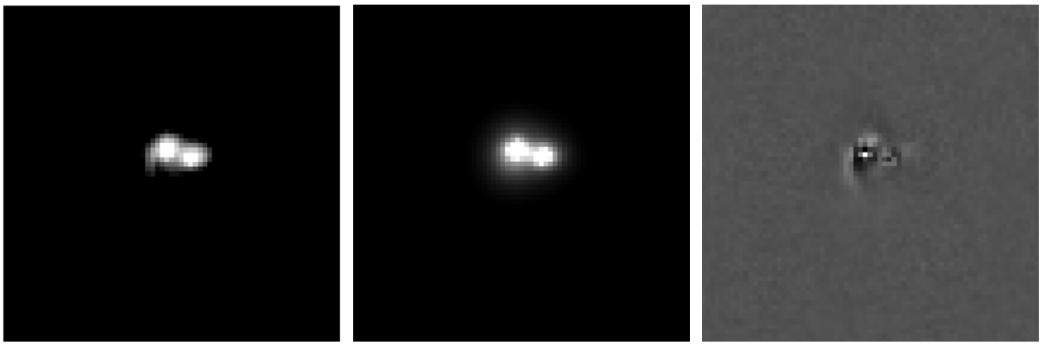

FIG. 6. The COSM J10020 source, the GALFIT produced model using fit stage (f), and the corresponding residual

IV. CONCLUSION

---

[1] Comerford. (2017) .An Active Galactic Nucleus Caught in the Act of Turning Off and On

[2] Courbin. (2006). The Host Galaxies of the Brightest Quasars: Gas-Rich Galaxies, Mergers, and Young Stars (incomplete citation)

[3] De Rosa. (2016). Unveiling multiple AGN activity in galaxy mergers

[4] cite ds9

[5] Frey. (2012). Two in one? A possible dual radio-emitting nucleus in the quasar SDSS J1425+3231

[6] Lambourne, Robert J. A. (2010). Relativity, Gravitation and Cosmology (Illustrated ed.). Cam-

bridge University Press. p. 222.

[7] Naab. (2006). Properties of Early-Type, Dry Galaxy Mergers and the Origin of Massive Elliptical Galaxies

[8] Wright (2006, PASP, 118, 1711).

[9] Ranganathan, A. (2004) "The Levenberg-Marquardt algorithm"

[10] Our summer research! Not sure how to cite this...

[11] Sersic, J. L. 1968, Atlas de galaxias australes (Cordoba: Observatorio Astronomico)

[12] tinytim manual